JCTC Journal of Chemical Theory and Computation

Approximate Inclusion of Triple Excitations in Combined Coupled Cluster/Molecular Mechanics: Calculations of Electronic Excitation Energies in Solution for Acrolein, Water, Formamide, and *N*-Methylacetamide

Kristian Sneskov,*,† Eduard Matito,‡,† Jacob Kongsted,§ and Ove Christiansen†

The Lundbeck Foundation Center for Theoretical Chemistry, Department of Chemistry, University of Aarhus, Langelandsgade 140, DK-8000 Aarhus C, Denmark, and Department of Physics and Chemistry, University of Southern Denmark, Campusvej 55, DK-5230 Odense M, Denmark

Received December 1, 2009

Abstract: Electronic excitation energies are often significantly affected by perturbing surroundings such as, for example, solvent molecules. Correspondingly, for an accurate comparison between theory and experiment, the inclusion of solvent effects in high-level theoretical predictions is important. Here, we introduce the CCSDR(3)/MM model designed for an effective, flexible, and accurate prediction of electronic excitation energies in solution. The method is based on a hybrid coupled cluster/molecular mechanics (CC/MM) strategy including interactions between a solute described by CC methods and a solvent described by polarizable MM methods. The CCSDR(3)/MM includes triples effects in a computational tractable noniterative fashion. The resulting approach allows for both high-accuracy inclusion of triples effects and inclusion of solute−solvent interactions with polarization effects, as well as being applicable for averaging over many solvent configurations derived from, for example, molecular simulations. We test the proposed model using as a benchmark the two lowest-lying valence singlet excitations ($n \rightarrow \pi^*$ and $\pi \rightarrow \pi^*$) of acrolein, formamide, and *N*-methylacetamide in aqueous solution as well as liquid water, demonstrating how a systematic inclusion of many different effects leads to good agreement with experimental values. In doing so we also illustrate the theoretical challenges involved when investigating UV properties of solvated molecules.

1. Introduction

In traditional quantum chemistry the major focus is on obtaining accurate energies and properties of isolated molecules. However, facing the experimental demand of *solvated* molecules while simultaneously requiring a flexible description of the one- and N-electron space poses a formidable challenge to modern quantum chemistry. Brute-force large-scale macromolecular calculations using high-accuracy ab initio theory are currently unfeasible for the most popular methods. Therefore, many schemes have been suggested in order to incorporate the perturbing effects of the surroundings in an approximate fashion.[1] One successful approach is based on the combined quantum mechanics/molecular mechanics (QM/MM) scheme,[2,3] which is also the approach we follow in this study. The QM part is defined as the chemically most important region. Therefore, invoking the well-established CC approximation is very satisfactory from a theoretical point of view. Combined with molecular mechanics, CC/MM allows for an accurate calculation of molecular properties. The development of CC/MM and similar methods is an active research area,[4–9] and in this work we consider further development of a strategy that includes polarization interac-

* To whom correspondence should be addressed. E-mail: sneskov@chem.au.dk. Fax: +4586196199.

† University of Aarhus.

‡ Present address: Institute of Physics, University of Szczecin, Wielkopolska 15, 70-451 Szczecin, Poland.

§ University of Southern Denmark.

10.1021/ct900641w
Published on Web 02/01/2010

tion between the QM and MM systems in the context of electronic excitation energy calculations.

The development of systematic CC models is an essential tool for the continuing investigation of molecular properties. Especially, these models serve as a reference for the computationally less expensive density functional theory (DFT) methods. In a series of papers,[10,11] the CC hierarchy of models—CCS, CC2, CCSD, and CC3—was established and tested in benchmark calculations.[12] It was also shown in past publications[13] how a noniterative analogue to CC3, CCSDR(3), could be designed providing excitation energies of seemingly similar quality to the CC3 model. The CCSDR(3) model is more appealing from a computational perspective as it incorporates effects due to triply excited configurations (henceforward denoted triples effects) in a *noniterative* fashion. The usefulness of CCSDR(3) and its ability to give very similar excitation energies to CC3 has recently been confirmed by Sauer et al. in an extensive study of medium-sized organic molecules.[14] The CC3 and CCSDR(3) methods were derived in a response theory framework. Related frameworks include equation-of-motion CC (EOM-CC)[15] (providing CCSD excitation energies identical to CC response theory) and symmetry adapted cluster/configuration interaction (SAC-CI).[16] Over the years a number of other approximate methods for inclusion of higher excitations in coupled cluster calculations of electronic excitations have been suggested also within these frameworks; see the lists in refs 8, 15, 17–19. A few of these have been successfully combined with a point-charge description of the surroundings and applied for instance in a study of the excited states of uracil[8] as well as in a retinal proteins investigation.[20] Here, we maintain the focus on CCSDR(3) and introduce the CCSDR(3)/MM model designed especially for the calculation of excitation energies in solution, and we stress the inclusion of polarization effects in addition to point charges.

In order to rigorously compare with experiment, it is mandatory to account for the effect of dynamics. This is routinely done by molecular dynamics (MD) or Monte Carlo sampling techniques, where the effect of the surroundings (here a solvent) is accounted for by a force field. Extracting conformations allows for an approximate sampling of the actual molecular environment by ultimately averaging the properties at hand over the conformations in a suitable fashion. This averaging requires many single-point calculations, emphasizing further the need for efficiency and thus the attractiveness of a noniterative triples approach like CCSDR(3) relative to an iterative approach.

Recently, some of us published[21] an extensive study of *s-trans*-acrolein, where the two lowest-lying singlet excitations were categorized in great detail. In the present study we use the same molecular geometries as in the former investigation, allowing us to directly ascertain the effects of triples in the aforementioned excitations energies. As a further test of the model, we also calculate electronic excitation energies and oscillator strengths of two amides, formamide and *N*-methylacetamide (NMA), demonstrating in the process the challenges involved in both the theoretical assignment of valence excitation energies as well as the direct comparison with experiment. Finally, we also investigate liquid water formerly studied by some of us without inclusion of triples.[22,23]

This paper is organized in the following way: In section 2.1 we outline the CC approximation and the use of CC response theory to calculate vertical excitation energies, including a definition of an excitation energy in CCSDR(3). In section 2.2, we briefly review the inclusion of solvent effects in the CC methodology, ending the section by defining the CCSDR(3)/MM model. In section 3, we outline the computational details, while we present the calculated values for solvated acrolein, formamide, NMA, and liquid water in section 4. Finally, section 5 contains the concluding remarks.

2. Theory

2.1. Excitation Energies in Coupled Cluster Theory. In conventional CC theory for isolated molecules the energy and amplitude equations take the form

$$E_{\mathrm{CC}}(t) = \langle \mathrm{HF}|\hat{H}\exp(\hat{T})|\mathrm{HF}\rangle \tag{1}$$

$$e_{\mu_i}(t) = \langle \mu_i|\exp(-\hat{T})\hat{H}\exp(\hat{T})|\mathrm{HF}\rangle = 0 \tag{2}$$

where $|\mathrm{HF}\rangle$ is the Hartree−Fock reference state, $\hat{T} = \sum_{\mu_i} t_{\mu_i}\hat{\tau}_{\mu_i}$ is the cluster operator, and $\langle\mu_i|$ is the excitation projection manifold. In the CCSD approximation $i = 1, 2$, such that the cluster operator is approximated to include only singles and doubles excitations $\hat{T} = \hat{T}_1 + \hat{T}_2$. The basic CC approaches are now textbook material, and we refer to ref 24 for further detail.

In response theory, the excitation energies for the exact wave function are found as poles of the linear response function. Similarly for approximate CC wave functions, the excitation energies are found by solving the CC response eigenvalue equations either for the right eigenvector

$$\mathbf{A}\mathbf{R}_k = \omega_k\mathbf{R}_k \tag{3}$$

or for the left eigenvector

$$\mathbf{L}_k\mathbf{A} = \mathbf{L}_k\omega_k \tag{4}$$

Here $\mathbf{A}$ is the CC asymmetric Jacobian

$$A_{\mu_i\nu_j} = \langle \mu_i|\exp(-\hat{T})[\hat{H}, \hat{\tau}_{\nu_j}]|\mathrm{CC}\rangle \tag{5}$$

Using this definition of the Jacobian, we note that the identification of the eigenvalues of the CC Jacobian as the excitation energies holds also for intermediate models such as CC2 and CC3.[25] Choosing the excitation vectors to be biorthonormal, $\mathbf{L}_i\mathbf{R}_j = \delta_{ij}$, the excitation energy can be written as

$$\omega_k = \mathbf{L}_k\mathbf{A}\mathbf{R}_k \tag{6}$$

A careful analysis of the order of the excitation energies in the CCSD model (see, for example, ref 11) reveals that the singles- and doubles-dominated excitations are correct through second and first order in the ground state fluctuation potential, respectively. In the CC3 and CCSDR(3) models,[11,13] on the other hand, the most important (in a perturbational sense) triples contributions are included such that both

models yield excitation energies correct to third and second order for the single- and double-dominated excitations, respectively.

In short, the iterative CC3 model is defined by invoking two approximations compared to the full CCSDT model: (1) the form of the singles and doubles amplitude equations is retained while the triples amplitude equation is restricted to the terms entering in lowest nonvanishing order in the fluctuation potential (second order), and (2) the singles are treated as zeroth-order parameters, thus implicitly accounting for orbital relaxation due to an external potential giving good response functions.

The main drawback of CC3 is the iterative N^7-scaling step motivating the development of the noniterative analogue: CCSDR(3).[13] The CCSDR(3) excitation energy is defined as

$$\omega = \mathbf{L}^{\mathrm{SD}}\mathbf{A}^{\mathrm{SD}}(t_1^*, t_2^*)\mathbf{R}^{\mathrm{SD}} + \sum_{\mu_i, i=1,2} L^{\mathrm{SD}}_{\mu_i} \sum_{\nu_3} \times \frac{\langle \mu_i|[\tilde{U}^*, \hat{\tau}_{\nu_3}]|\mathrm{HF}\rangle\langle \nu_3|[\tilde{U}^*, \hat{R}_2^{\mathrm{SD}}] + [\tilde{U}^*, \hat{R}_1^{\mathrm{SD}}], \hat{T}_2^*|\mathrm{HF}\rangle}{\omega_{\nu_3} - \omega^{\mathrm{SD}}} + \sum_{\mu_2} L^{\mathrm{SD}}_{\mu_2}\langle \mu_2|[[\hat{U}, \hat{R}_1^{\mathrm{SD}}], \hat{T}_3^*]|\mathrm{HF}\rangle \quad (7)$$

Here ω^{SD} is the CCSD excitation energy while $\mathbf{L}^{\mathrm{SD}}$ and $\mathbf{R}^{\mathrm{SD}}$ are CCSD response eigenvectors and

$$\hat{R}_i^{\mathrm{SD}} = \sum_{\nu_i} R^{\mathrm{SD}}_{\nu_i}\hat{\tau}_{\nu_i} \quad \text{for } i = 1, 2 \quad (8)$$

In eq 7 we have implied a partitioning of the Hamiltonian into the Fock operator and the fluctuation potential $\hat{H} = \hat{F} + \hat{U}$.

$\tilde{U}$ is in turn a T_1 similarity transformed operator according to

$$\tilde{U} = \exp(-\hat{T}_1)\hat{U}\exp(\hat{T}_1) \quad (9)$$

$\mathbf{A}^{\mathrm{SD}}(t_1^*, t_2^*)$ is the CCSD Jacobian constructed with the triples-corrected amplitudes defined as

$$t^*_{\mu_i} = t^{\mathrm{SD}}_{\mu_i} + \frac{\langle \mu_i|[\tilde{H}, \hat{T}_3]|\mathrm{HF}\rangle}{\omega_{\mu_i}} \quad (10)$$

where $\hat{T}_3$ is constructed on-the-fly from the CCSD amplitudes according to

$$t_{\mu_3} = -\frac{\langle \mu_3|[\tilde{U}, \hat{T}_2]|\mathrm{HF}\rangle}{\omega_{\mu_3}} \quad (11)$$

where a canonical representation has been implied. ω_{μ_i} contains orbital energy differences between occupied and virtual orbitals. In the CCSDR(3) approximation, a one-step perturbative correction is applied while this same correction is performed until convergence in the CC3 model.

In passing, we note that the excitation energies are no longer found as poles of any response functions due to the perturbational nature of CCSDR(3).

2.2. Environmental Effects. In order to include the effects of a surrounding environment, in the present case a solvent, a set of interaction terms are augmented to the vacuum energy expression. This implies a partitioning of the terms into a vacuum and a solvent part. This partitioning carries over to the Jacobian such that the total Jacobian may be written as

$$\mathbf{A}^{\mathrm{tot}} = \mathbf{A}^{\mathrm{vac}} + \mathbf{A}^{\mathrm{solv}} \quad (12)$$

where the form of $\mathbf{A}^{\mathrm{vac}}$ is still given by eq 5, but using the in-solution amplitudes, while the solvent Jacobian is given by

$$A^{\mathrm{solv}}_{\mu_i\nu_j} = \langle \mu_i|\exp(-\hat{T})[\hat{T}^g, \hat{\tau}_{\nu_j}]|\mathrm{CC}\rangle + \langle \mu_i|\exp(-\hat{T})\hat{T}^{g\nu_j}|\mathrm{CC}\rangle \quad (13)$$

The effective operators $\hat{T}^g$ and $\hat{T}^{g\nu_j}$ are introduced as

$$\hat{T}^g = \sum_p \lambda_p\hat{X}_p + \sum_q \gamma_q(\langle \Lambda|\hat{Z}_q|\mathrm{CC}\rangle\hat{Y}_q + \langle \Lambda|\hat{Y}_q|\mathrm{CC}\rangle\hat{Z}_q) \quad (14)$$

$$\hat{T}^{g\nu_j} = \sum_q \gamma_q(\langle \Lambda|[\hat{Z}_q, \hat{\tau}_{\nu_j}]|\mathrm{CC}\rangle\hat{Y}_q + \langle \Lambda|[\hat{Y}_q, \hat{\tau}_{\nu_j}]|\mathrm{CC}\rangle\hat{Z}_q) \quad (15)$$

where we have applied the auxiliary state $\langle\Lambda| = (\langle \mathrm{HF}| + \sum_{i\mu_i}\bar{t}_{\mu_i}\langle \mu_i|)\exp(-\hat{T})$. The notation used here is very general and is used due to the flexibility, allowing for a simultaneous description of the CC/MM model as well as the more simplified dielectric continuum description of the surroundings, denoted the CC/DC model.[26] In the latter implicit description of the solvent, the solute is placed in a (spherical) cavity surrounded by a continuum described by a dielectric constant. This may in eqs 14 and 15 be represented by dropping the term with the summation over p and letting the sum over q represent a multipole expansion for the charge distribution of the solute, thus implying that in the case of CC/DC $\hat{Y}_q = \hat{Z}_q$ are related to multipole operators. The explicit CC/MM model describes the surroundings using a molecular mechanics force field such that the effective operators in eqs 14 and 15 describe the electrostatic interaction between solute and solvent. Thus, the sum over p is related to the partial charges distributed in the MM region while the effects of polarization are incorporated in the sum over q. In both cases concrete expressions of these operators can be found in ref 5. We emphasize that the appearance of the solvent Jacobian in eq 12 is a direct consequence of the explicit inclusion of polarization effects thorugh the polarizabilities. If no polarization is included (e.g., a simple point-charge model), no extra term in the Jacobian appears provided that the partial point-charges have been absorbed into the Hamiltonian, and it would be sufficient to use the in-solution amplitudes in the expression for the vacuum Jacobian. Clearly, this more widespread approximation leads to much simpler equations, but here it is not taken as default.

In a straightforward CC3 approach, one would iteratively introduce the effects of triples in both the description of the solute and the solute−solvent interaction terms. However, it is currently intractable to perform such high-accuracy

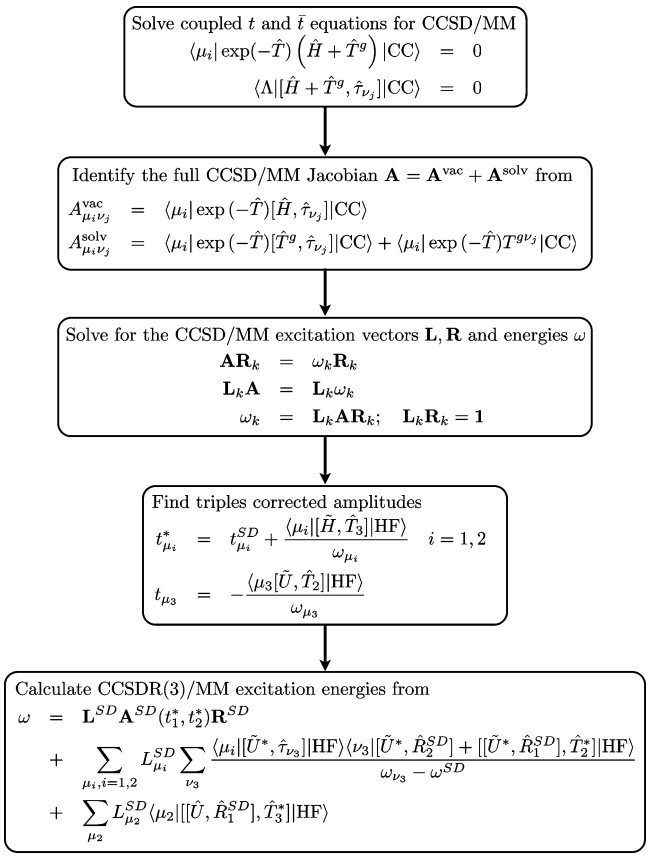

Figure 1. Overview of the proposed CCSDR(3)/MM model. See the text for definitions.

triples corrections, and we herein propose a CCSDR(3)/MM model which explicitly incorporates triples corrections in a noniterative fashion for the solute only, while the solvent−solute interaction is essentially described at the CCSD/MM level. Thus, we use the CCSD/MM vectors, in place of the vacuum CCSD vectors, as well as the triples-corrected operators in eq 7 and obtain a highly flexible description of the excitation energies of a molecule in a solvent. The proposed CCSDR(3)/MM model is illustrated in Figure 1.

3. Computational Details

The theory outlined in the previous section is here illustrated using various molecular systems: acrolein in aqueous solution, formamide in aqueous solution, NMA in aqueous solution, and liquid water. The effects of introducing a water solvent are incorporated by using molecular mechanics. The strategy behind the current QM/MM implementation is as follows: First, we determine partial charges and polarizabilites to be placed in the MM region. The latter are the key ingredient for determining induced dipoles allowing for a description of polarization between the two subsystems. Using these parameters a force field is constructed and subsequently applied in a molecular dynamics (MD) simulation using suitable settings for the macroscopic parameters (T, V, etc.), thus effectively simulating the effects of a nonzero temperature. From this simulation a set of 120 uncorrelated configurations, sufficient to obtain converged excitation energies,[21] is extracted and stored independently. Next we perform 120 independent QM/MM calculations until certain convergence criteria are satisfied; e.g., in the present implementation the induced dipoles are converged. Finally, we perform a statistical analysis of the 120 different excitation energies and oscillator strengths in order to estimate a number for the final valence excitation energy.

However, a straightforward averaging procedure over the different excitation energies ordered with respect to energy is problematic. Indeed, the excitations often become heavily mixed, as discussed in the next section. Thus, often it is very difficult to estimate a single vertical transition energy using a simple averaging technique. However, we may still construct a spectrum of the solvated sample, and to do so we introduce a broadening of the stick spectrum. We do this by assigning an explicit broadening using for each state of each configuration a Gaussian function of a finite width[23] (for simplicity fixed to 0.1 eV for all states in all molecules) designed such that the integral of each Gaussian gives the oscillator strength. We note that this identification is somewhat arbitrary and may be altered at our convenience if better resemblance to the experimental spectrum is strived for. The final spectrum will thus consist of a superposition of these distributions appropriately scaled by the inverse of the number of configurations to describe the averaged spectrum. Thus, the integral of the superposed Gaussians will give the averaged oscillator strength if one well-separated state is studied. This procedure has the advantage of giving a well-defined spectrum also in the case of mixed states, where the calculation of an average oscillator strength is problematic. The absorption strengths reported in some figures are the oscillator strength distributions as defined above. Finally, we compare the position of the band maximum to experiment, and if the experimental spectrum is readily available, we include a (scaled) version for ease of comparison. Note that we do not aim for exact agreement between the theoretical and experimental spectra, since we do not incorporate effects like vibronic coupling known to potentially change the appearance of the spectrum.

A basis set investigation[21] revealed that the basis set aug-cc-pVDZ[27] is sufficient for the description of the excitation energies of interest in acrolein. Similarly, for the NMA molecule we also apply the aug-cc-pVDZ basis, while we further augment diffuse functions (d-aug-cc-pVDZ) for the description of formamide. Finally, for the smaller water molecule the large d-aug-cc-pVTZ basis set is used.[22] We aim solely at improving the N-electron space, while the choice of basis set is kept fixed. All calculations use frozen 1s orbitals for the heavy atoms. Furthermore, a spherical cutoff radius of 12 Å (corresponding to the nearest 230−240 water molecules) is applied in all the QM/MM calculations. The geometry of the QM molecule(s) were all found using B3LYP/aug-cc-pVTZ accounting for the bulk solvent effects by using the familiar polarizable continuum model (PCM). The partial charges and polarizabilities were also determined at the B3LYP/aug-cc-pVTZ level of theory using the CHELPG procedure[28] and the LOPROP approach,[29] respectively. The Lennard-Jones parameters were taken from refs 30 and 31. The applied force fields were SPCpol for acrolein, formamide, and NMA, while TIP3P was used for liquid water. Further details on the MD simulations may be found

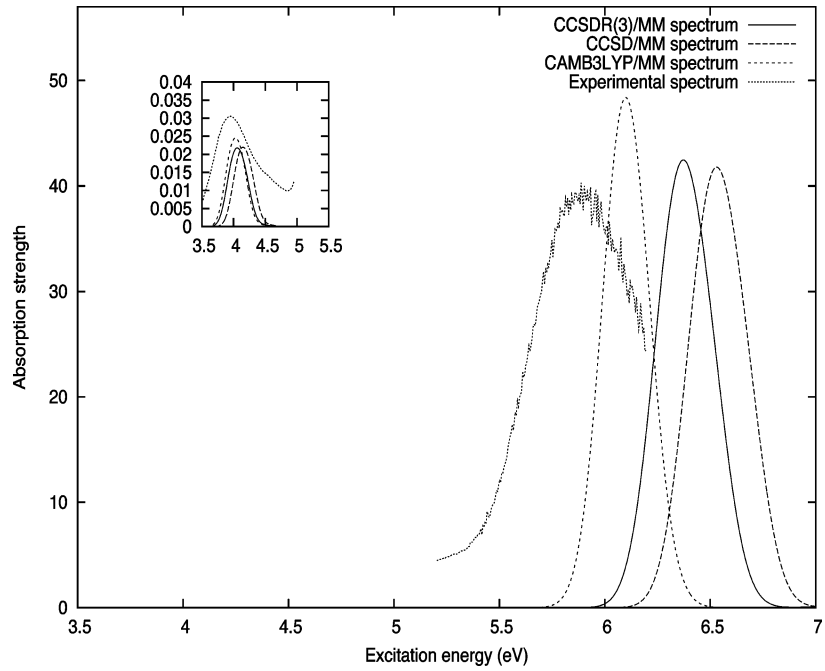

Figure 2. Acrolein spectrum n → π^* and $\pi \rightarrow \pi^*$ calculated at the CCSD/MM, CCSDR(3)/MM, and CAM-B3LYP/MM level of theory. For completion, an inset of the spectrum on a different scale is included. Also included is a scaled version of the experimental spectrum. See the text for details.

in ref 21. All vacuum calculations presented in the following are based on B3LYP/aug-cc-pVTZ-optimized geometries, as was also the case in the previous study of acrolein.[21]

The MD simulations have been performed using the MOLSIM program package.[32] The distributed polarizabilities were determined using the MOLCAS program.[33] The used QM/MM scheme was described in refs 34 and 35 and implemented in the DALTON quantum chemistry package.[36] The MIDASCPP program[37] has been used for preparing the input and the final statistical analysis of the data. Finally, the Gaussian 03 package[38] has been used for both finding the partial charges as well as optimizing the singlet excited states in order to estimate zero-point vibrational corrections to the energy.

4. Results

4.1. Acrolein in Aqueous Solution. As a first application of the CCSDR(3)/MM model, we make a thorough investigation of the two lowest-lying excitation energies of the acrolein molecule. In ref 21 it was found that the CAM-B3LYP functional compared well with findings using CCSD, with the obvious benefit of being much less computationally demanding, thus allowing for full QM calculations with as much as 12 water molecules in the QM part of the system. It was shown that this was indeed necessary in order to converge the $\pi \rightarrow \pi^*$ excitation energy, suggesting that this transition is dominated by nonelectrostatic contributions. In that paper, there is still small discrepancies between the converged CAM-B3LYP MD QM/MM(SPCpol) 12 (H_2O)QM and the experimental findings; these are the discrepancies we target by including triples. However, carrying out calculations on such large QM regions is not attractive, and the idea would thus be to estimate the contribution from a large QM solvent shell from CAM-B3LYP calculations. This will be clarified in the following.

Before this we note that it is not straightforward to compare theoretical and experimental values. First of all, in experiments a transition between electronic states is characterized by a relatively broad peak, making it difficult to directly deduce a vertical excitation energy; one has to assume this corresponds to the point of maximum absorption. As noted in ref 21, it is problematic to determine this maximum for the $\pi \rightarrow \pi^*$ transition in acrolein uniquely. As is clear from the experimental spectrum in Figure 2, the *point* of maximum absorbance is better described as an *interval* of maximum of absorbance with a length of approximately 0.5 eV, hence representing a substantial uncertainty considering the high level of theory used in this work. Second, effects due to intramolecular vibrations and the vibrational structure of the band are not included in the theoretical predictions.

With these words of caution we proceed by reporting the n → π^* excitations in Table 1. We note that this excitation is already fairly well described at the CCSD level. In Table 1 we also report the shifts referenced to acrolein in vacuum as well as the experimental and calculated values from ref 21.

It is seen that triples effects serve to lower the absolute values by about 0.1 eV, while the solvent shift is essentially unaltered. The shift is in good agreement with experiment, while the absolute value still is in disagreement by approximately 0.1 eV. Considering that this discrepancy is also present in the case of the vacuum transition, it is most probably not due to an insufficient solvent description but is related to the vibrational structure of the band not included in these calculations. This point is emphasized when considering the previously mentioned CAM-B3LYP calcula-

Table 1. Overview of the Reported Excitation Energies for the n → π* and π → π* Excitation Energies (in eV) of Acrolein in Vacuum and Water Solution and Corresponding Solvent Shifts[a]

ref	method	$^{vac}E_{ex}^{n\rightarrow\pi^*}$	$^{liq}E_{ex}^{n\rightarrow\pi^*}$	$\Delta E_{ex}^{n\rightarrow\pi^*}$	$^{vac}E_{ex}^{\pi\rightarrow\pi^*}$	$^{liq}E_{ex}^{\pi\rightarrow\pi^*}$	$\Delta E_{ex}^{\pi\rightarrow\pi^*}$
Aidas et al.[21]	CAM-B3LYP MD QM/MM(SPCpol) 0 (H_2O)QM	3.78	4.14	0.36	6.41	6.13	−0.28
	CAM-B3LYP/MM(SPCpol) 2 (H_2O)QM		4.04	0.26		6.07	−0.34
	CAM-B3LYP/MM(SPCpol) 12 (H_2O)QM		4.04	0.26		5.95	−0.46
present work	CCSD MD QM/MM(SPCpol) 0 (H_2O)QM	3.91	4.16	0.25	6.87	6.54	−0.33
	CCSD/MM(SPCpol) 2 (H_2O)QM		4.15	0.24		6.51	−0.36
	CCSDR(3)/MM(SPCpol) 0 (H_2O)QM	3.81	4.07	0.26	6.73	6.38	−0.35
	CCSDR(3)/MM(SPCpol) 2 (H_2O)QM		4.06	0.25		6.35	−0.38
	CCSDR(3)/MM(SPCpol) 0 (H2O)QM + E_{nonel} (CAM-B3LYP-SPCpol)		4.08	0.27		6.22	−0.51
expt[21]		3.69	3.94	0.25	6.41	5.90	−0.52

[a] Also included are the values calculated in a related previous study as well as experimental results.

tions on acrolein,[21] which are also included in Table 1. Explicitly, it is noted that the n → π* has no significant contribution from water molecules when these are explicitly included in the QM part.

Finally, we note that a recent CASSCF//CASPT2 investigation[39] gave vacuum and solvated n → π* transition energies of 3.77 and 3.96 eV, respectively, thus providing a shift in good agreement with those presented Table 1.

We now turn our attention to the π → π* excitation in Table 1. Comparing the CCSDR(3) and CCSD calculated values, we see a larger effect of triples excitations for this state, resulting in a lowering of approximately 0.2 eV for the absolute excitation energy. As for the n → π* transition the impact of triples is close to being canceled when considering solvent shifts rather than absolute values of the excitation energies.

Focusing on the shifts we see that, compared to the experimental values, the CCSDR(3) values are still somewhat off, suggesting that the remaining error is not due to triples effects but rather due to the nonelectrostatic nature of the interaction between this excited state and the solvent.

We estimate the size of this effect by taking the difference between two CAM-B3LYP calculated excitation energies. We subtract the excitation energy found with a QM region including only acrolein itself from a large-scale QM calculation (12 water molecules treated quantum mechanically; see ref 21 for a justification for the size of the QM system). This contribution will be added to the excitation energy found using CCSDR(3) including also only acrolein in the QM region. The results are included in Table 1 and this extra contribution is labeled E_{nonel}(CAM-B3LYP-SPCpol). For completion, we have included the n → π* nonelectrostatically corrected excitation energies. We see that the shifted values with the nonelectrostatic correction are almost identical to the experimental values. Though this final agreement between theory and experiment is comforting, one should not overemphasize this. Especially, we note that since the CCSD/MM and CCSDR(3)/MM solvent shifts only differ by approximately 0.02 eV we could have performed a similar estimate for the CCSD/MM excitation energy shifts. Large-scale CAM-B3LYP calculations turned out in this case to be a very efficient and economical way to estimate the nonelectrostatic effects not included in the (purely electrostatic) interaction between the QM and MM subsystems.

Now changing our focus to the absolute excitation energies in the gas phase, we see that they are still alluding us by almost 0.3 eV as compared with experiment. This deviation might suggest that the remaining contribution is not connected with the lack of electron correlation but rather has to do with geometry effects (all QM calculations are performed on B3LYP-optimized structures as in ref 21) and the lack of vibrational structure of the band (including zero-point energy contributions).

Table 2. Lowest-Lying Singlet Excitation Energies (in eV) for Water in Vacuum and the Liquid Phase as Well as the Corresponding Solvatochromic Shift Calculated in a Hierarchy of CC Methods as Well as with DFT

ref	method	$^{vac}E_{ex}^{\tilde{A}}$	$^{liq}E_{ex}^{\tilde{A}}$	$\Delta E_{ex}^{\tilde{A}}$
present work	B3LYP/MM	6.90	7.43	0.53
	CAM-B3LYP/MM	7.13	7.72	0.59
	CC2/MM	7.25	7.86	0.61
	CCSD/MM	7.62	8.25	0.63
	CCSDR(3)/MM	7.61	8.25	0.64
expt[42]		7.4	8.2	0.8

Consequently, we have estimated the zero point vibrational contribution (ZPVC) to the lowest-lying singlet excited state for acrolein in a vacuum. Using CIS/6-311++G(d,p) to optimize the excited state structure followed by an evaluation of the vibrational frequencies, we estimate this contribution to be −0.11 eV, which combined with the CCSDR(3) vacuum excitation energy (3.81 eV − 0.11 eV = 3.70 eV) is in excellent agreement with experiment (3.69 eV). The vibrational structure of the second excited state is noteworthy more complex, as also noted elsewhere.[40] However, using the vibrational frequencies available in ref 40 at the CASSCF/cc-pVTZ level of theory as well as performing an analogous calculation for the ground state (see ref 40 for details on the active space) we are able to estimate a ZPVC of approximately −0.14 eV, which combined with the CCSDR(3) calculated excitation energy (6.73 eV − 0.14 eV = 6.59 eV) is in satisfactory agreement with experiment (6.41 eV) when recalling the very diffuse nature of the experimental band. The fact that CAM-B3LYP is in such good agreement *without* inclusion of these effects is perhaps a little worrisome but nevertheless very remarkable.

On the basis of oscillator strengths from CCSD/MM calculations, we have also constructed CCSDR(3)/MM spectra for acrolein in aqueous solution. In Figure 2 the CCSD/MM as well as CCSDR(3)/MM spectra are given. We recall that the spectra are calculated by representing each

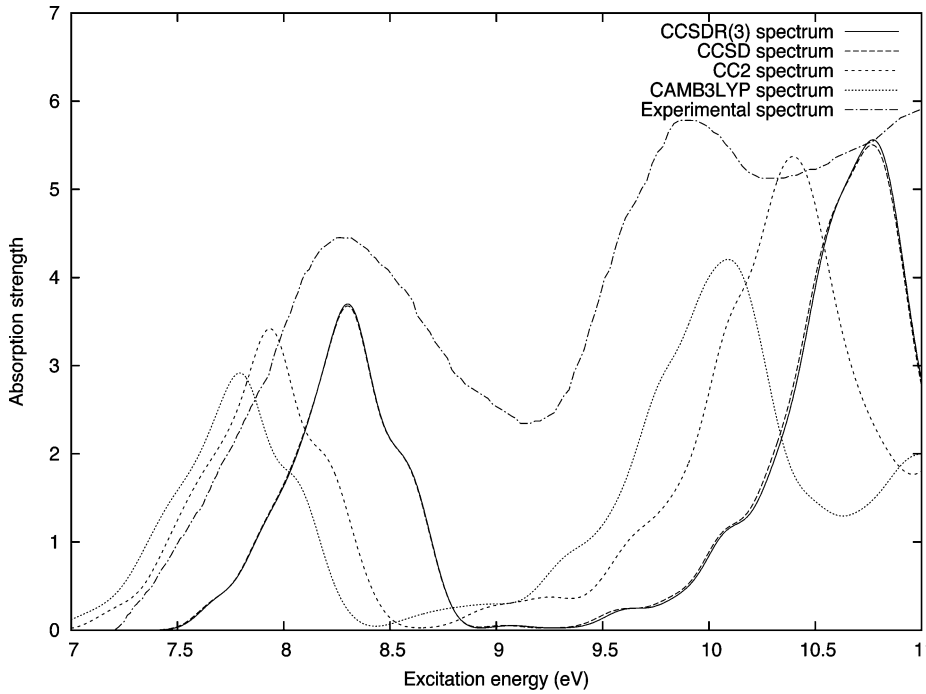

Figure 3. Water spectrum, with the lowest-lying excitations in water averaged over 120 configurations calculated at CC2/MM, CCSD/MM, CCSDR(3)/MM, and CAM-B3LYP/MM levels of theory. Also included is a scaled version of the experimental spectrum.

Table 3. Overview of the Reported Excitation Energies for the n → π^* and $\pi \rightarrow \pi^*$ Excitation Energies (in eV) of Formamide in Vacuum and Water Solution and Corresponding Solvent Shifts[a]

method	$^{vac}E_{ex}^{n\rightarrow\pi^*}$	$^{liq}E_{ex}^{n\rightarrow\pi^*}$	$^{vac}E_{ex}^{\pi\rightarrow\pi^*}$	$^{liq}E_{ex}^{\pi\rightarrow\pi^*}$
CAM-B3LYP/MM(SPCpol)	5.59	5.97	7.69	7. 45[b]
CCSD/MM(SPCpol)	5.70	6.15	7.58	7.16
CCSDR(3)/MM(SPCpol)	5.69	6.13	7.69	7.09
Expt[43,48]	5.8	5.2−5.9	7.4	>6.5

[a] Also included are the experimental results. [b] Assignment based on spectrum.

state for each structure by a Gaussian whose integral is proportional to the oscillator strength.

It is evident that the inclusion of triples red-shifts the band. Due to symmetry reasons the n → π^* transitions in carbonyl compounds are typically weak and it is therefore of no surprise that the oscillator strength (not given explicitly here) of the n → π^* excitation is approximately 3 orders of magnitude smaller than for the $\pi \rightarrow \pi^*$ transition demonstrated by the inset in Figure 2. Finally, we have also included the CAM-B3LYP/MM spectrum in Figure 2.

4.2. Liquid Water. We have also investigated the electronic spectrum of water with the CCSDR(3)/MM model. We will focus only on the lowest-lying excitation—in the literature often labeled $\tilde{A}$—since this, as discussed in ref 23, is well-separated (by approximately 1 eV) from the remaining ones. In Table 2 we show the lowest-lying excitation energy calculated for liquid water modeled explicitly by one water molecule being treated quantum mechanically while the remaining ones are treated classically. We see that for this system DFT gives far too low excitation energies stemming from the partly Rydberg nature of the electronic transitions in water. This is not surprising, since the approximate exchange functionals used in DFT contain spurious electronic self-interaction terms which previously have been noted to give too low Rydberg excitation energies.[41] On the contrary, full inclusion of doubles in the CCSD model markedly increases the excitation energies while the final inclusion of triples has only fine-tuning effects of approximately 0.03 eV. This conclusion is even more apparent in Figure 3, where we have superimposed four theoretical spectra at the CC2/MM, CCSD/MM, CCSDR(3)/MM, and CAM-B3LYP/MM level of theory, respectively, as well as a recreation of the experimental spectrum.[42] Going from CC2 to CCSD clearly results in a blue-shifting of the bands, while inclusion of triples effects leaves an almost identical spectrum compared to CCSD. This is as expected considering the electronic structure of water. We also note that the CAM-B3LYP spectrum is red-shifted as compared to the CC2 spectrum, thus emphasizing the underestimation of the excitation energies of water when described by DFT.

In experiment, the location of the two lowest-lying excitations is approximately 8.2 eV in good agreement with the calculated $\tilde{A}$ excitation energy.

4.3. Formamide in Aqueous Solution. Drawing on the conclusions from the acrolein investigation, we apply the CCSDR(3)/MM model on formamide. We especially compare CCSDR(3)/MM and CAM-B3LYP results and the resulting spectra. In most amides the spectrum is characterized by, besides a multitude of Rydberg transitions, a very intense $\pi \rightarrow \pi^*$ transition and a very weak n → π^* transition. Upon introduction of a polar solvent (e.g., water) these two valence transitions are red- and blue-shifted, respectively. Consequently, the weak n → π^* transition is hidden below the much stronger $\pi \rightarrow \pi^*$ band, naturally complicating a thorough characterization of this vertical transition. Therefore, we here perform an extensive

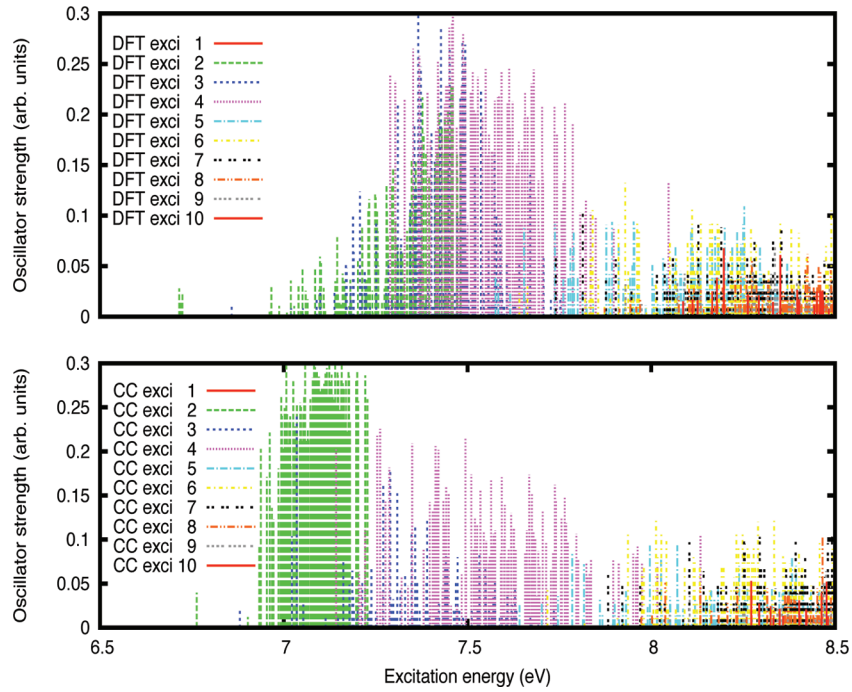

Figure 4. Distribution of the 10 lowest-lying excitation energies in 120 different configurations of formamide solvated in water described using CCSDR(3)/MM and CAM-B3LYP/MM, respectively.

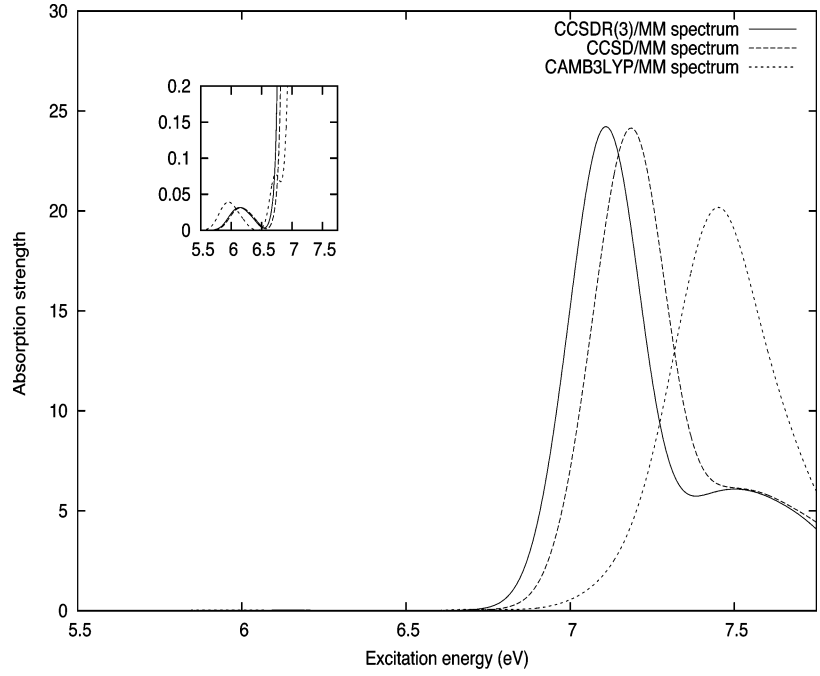

Figure 5. CCSD/MM, CCSDR(3)/MM, and CAM-B3LYP/MM spectra of aqueous formamide with insets in different scale to illustrate the weak n → π^* transition.

analysis of the degree of mixing between the excited states energies and take measures accordingly when estimating the valence excitation energies. In doing so we also hope that the technical challenges involved in simulating realistic spectra of solvated samples are illuminated.

In Table 3 we have included the calculated excitation energies of the lowest-lying valence excitations in formamide. For the n → π^* excitation there is a discrepancy between the calculated vertical excitation energy and the experimental energy of maximum absorption of approximately 0.1 eV. Given that inclusion of triples effects takes us further away from the experimental value, we conclude that the remaining effects are not due to dynamical correlation. Similarly, for the $\pi \rightarrow \pi^*$ transition the CC and DFT models are in disagreement with experiment by approximately 0.3 eV, where we again see that inclusion of triples does not improve the description of the excitation energy as compared to experiment. On the basis of the acrolein study it seems likely that the remaining disagreement between theory and experiment is due primarily to ZPVC effects. Actual calculations, implying yet another excited state optimization, is beyond the scope of this paper.

Table 4. Overview of the Reported Excitation Energies for the n → π* and π → π* Excitation Energies (in eV) of NMA in Vacuum and Water Solution and Corresponding Solvent Shifts[a]

method	$^{vac}E_{ex}^{n\rightarrow\pi^*}$	$^{liq}E_{ex}^{n\rightarrow\pi^*}$	$^{vac}E_{ex}^{\pi\rightarrow\pi^*}$	$^{liq}E_{ex}^{\pi\rightarrow\pi^*}$
CAM-B3LYP/MM(SPCpol)	5.75	6.15	6.41	7. 17[c]
CCSD/MM(SPCpol)	5.88	6.30	6.43	7. 05[c]
CCSDR(3)/MM(SPCpol)	5.84	6.27	6.29	6. 96[c]
expt[46,49]	N/A	5. 54[b]	6.81	6.67

[a] Also included are the experimental results. [b] Estimated using solvent difference techniques. [c] Assignment based on spectrum in Figure 7.

Instead we focus on the analysis of the CCSDR(3)/MM results. In Figure 4 we show the distribution of the excitation energies in the 120 different configurations. In this figure we do not directly observe the weak n → π* transition since (1) it is well-separated (lower) in energy from the rest and (2) the oscillator strengths are several orders of magnitude smaller than the other valence excitation. Therefore, it is straightforward to find a point of maximum absorption by averaging the lowest-lying excitation energy in all the configurations, thus obtaining a value of 6.13 eV. However, the second lowest excitation energy does not always correspond to a π → π* transition (based on the size of the oscillator strength). That being said, the mixing only occurs for a relatively few number of configurations and it is still possible to estimate a π → π* excitation energy by an explicit averaging over the second-lowest excitation energy obtaining a value of 7.09 eV. Also depicted in Figure 4 is a similar analysis using CAM-B3LYP as opposed to CCSDR(3) for the description of the QM region. We observe that for CAM-B3LYP it is essentially impossible to deduce a pure π → π* transition, as the excitation energies are heavily mixed, preventing any meaningful averaging. Finally, we may construct a full spectrum; indeed, one might argue that it is the only viable option in cases where the Rydberg transitions and valence transitions are so heavily mixed. The final spectra for CCSD/MM, CCSDR(3)/MM, and CAM-B3LYP/MM are shown in Figure 5. We note that a peak corresponding to the n → π* is located at approximately 6.1 eV for CCSDR(3)/MM and at 6.0 eV for CAM-B3LYP/MM. The π → π* excitation energy is peaked at approximately 7.1 eV for CCSDR(3)/MM and 7.5 eV for CAM-B3LYP/MM. Also, in the CAM-B3LYP/MM spectrum we observe a small kink on the low-energy side of the strong π → π* band. In the experimental spectrum[43] a band in the tail of the π → π* band is observed from 5.2 to 5.9 eV and assigned to the n → π* transition. This is somewhat lower than our predicted values. For the π → π* excitation energy no experimental details are available, except that it is located above 6.5 eV, as predicted by both models. Finally, we note the application of other methods for calculating vertical excitation energies and shifts. In particular, a macroscopic continuum CASSCF//CASPT2 investigation[44] gave n → π* and π → π* vertical transition energies of 5.54 and 6.95 eV, respectively, while a Monte Carlo INDO-CIS calculation[45] provided extrapolated solvent shifts of 0.2 eV and −0.1, respectively.

4.4. NMA in Aqueous Solution. As a further test of CCSDR(3)/MM, we investigate the spectrum of a slightly more complicated amide: *N*-methylacetamide (NMA). In Table 4 we have included the calculated vacuum excitation energies of the lowest-lying valence excitations. The n → π* excitation energy is not available in experiment while the π → π* excitation energy peaks at 6.81 eV.

In Figure 6 we demonstrate the distribution of the lowest-lying excitations in NMA for all 120 configurations using both CCSDR(3) and CAM-B3LYP. Contrary to the case of formamide, we see that not even CCSDR(3) offers a way to easily estimate a π → π* excitation energy. We also observe that only the CC calculations reveal a degree of mixing

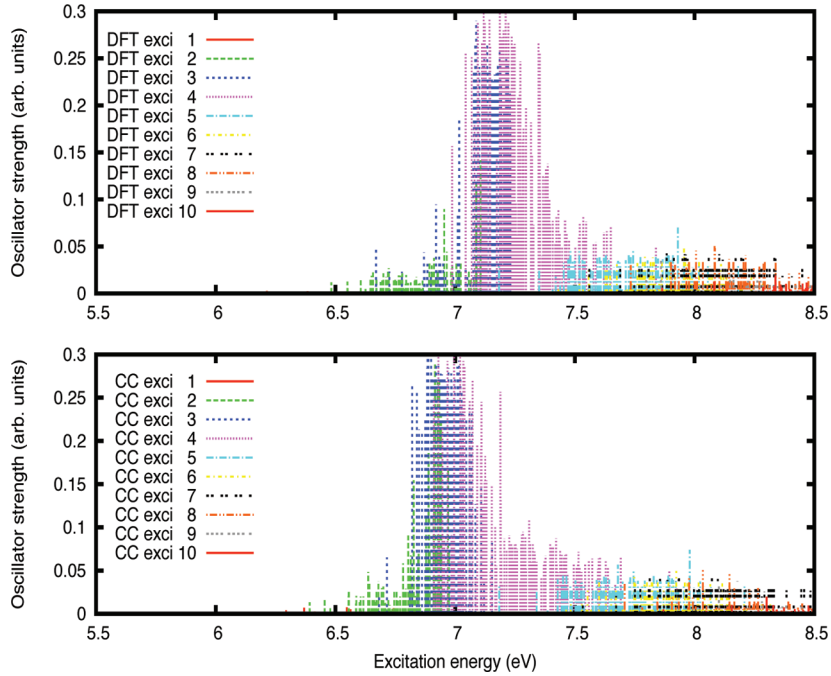

Figure 6. Distribution of the 10 lowest-lying excitation energies in 120 different configurations of NMA solvated in water described using CCSDR(3)/MM and CAM-B3LYP/MM, respectively.

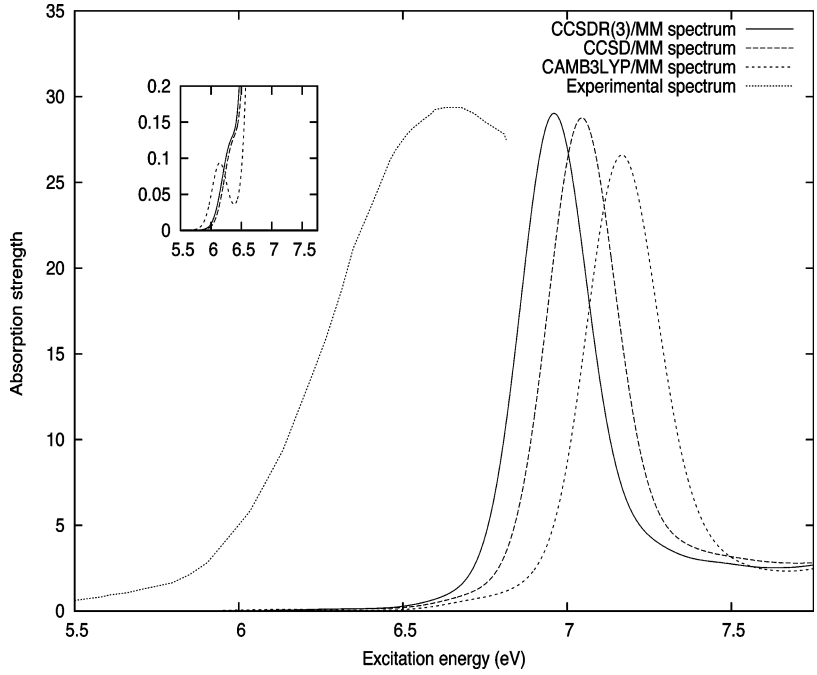

Figure 7. CCSD/MM, CCSDR(3)/MM, and CAM-B3LYP spectra of aqueous NMA with insets in different scale to illustrate the weak n → π^* transition. Also included is a scaled version of the experimental spectrum.

between the weak n → π^* and the higher-lying transitions. At a first inspection, the picture provided by DFT (a well-separated n → π^* transition) may seem more comforting. However, as hinted to in the previous section, in experiment it is extremely difficult to estimate the n → π^* excitation energy of amides, as it is essentially hidden (oscillator strength of the order 0.0025 was reported in fine agreement with the values presented here) under the much stronger π → π^* band. The complicated photoabsorption of NMA is not apparent from the DFT calculations but is conveyed nicely in the CC calculations. Finally, we must be cautious especially when analyzing the DFT spectrum since, as mentioned in the water investigation, DFT has problems describing excitations that are Rydberg in nature.

We have constructed the final spectrum of NMA in aqueous solution shown in Figure 7 and from this we may estimate approximate band maxima. In experiment a band with a maximum at 6.7 eV is assigned to the π → π^* transition. This is in agreement with the CCSDR(3)/MM spectrum in Figure 7, which has a strong bandwidth at approximately 6.9 eV. When no triples effects are included (e.g., the CCSD/MM model) we observe a slight overestimation of this transition as compared to experiment while the CAM-B3LYP/MM calculations seem to overestimate the position of this band even further. In experiment, a value for the n → π^* excitation energy has been estimated (5.5 eV) using nonpolar → polar solvent difference techniques, but it was also noted that these methods usually provide values that are too low.[46] From Figure 7 we see a very weak shoulder at around 6.3 eV. For the spectrum calculated using CAM-B3LYP/MM we see, as mentioned above, that the n → π^* is more separated from the strong π → π^* transition as compared to the CC calculation. For completeness we have included a recreation of the experimental spectrum.[46]

In the literature other calculations of vertical excitation energies and shifts have been reported. As for the formamide molecule we note that a macroscopic continuum CASSCF//CASPT2 calculation[44] gave a n → π^* excitation energy of 5.56 eV and a π → π^* energy of 6.60 eV. Finally, Monte Carlo INDO-CIS extrapolated solvent shifts have been reported[47] for the considered states of approximately 0.22 and −0.15 eV, respectively, both shifts being somewhat lower than the values reported in Table 4.

5. Conclusions

We have introduced the CCSDR(3)/MM model, a noniterative method to incorporate triples effects in a QM/MM calculation. We have tested it on four model systems: *s-trans*-acrolein, formamide, and NMA in aqueous solution and liquid water. For the former system we perform a thorough investigation of the two lowest-lying valence singlet excitation energies. For the n → π^* we obtain perfect agreement with experiment for the solvent shift. The vacuum energy comes close to experiment only when including ZPVC. The π → π^* proves a little more troublesome as it contains a large nonelectrostatic contribution requiring a large QM region. This was estimated using CAM-B3LYP, ultimately yielding good agreement between theory and experiment for the solvent shift. Ultimately, the effects of triples in acrolein on the lowest singlet excitation energies correspond to approximately −0.1 and −0.15 eV. The investigation of two amides (formamides and NMA) shows us that it is not straightforward to include the effects of dynamics in a simple averaging procedure, as the individual excitation energies tend to mix in the different configurations. While CCSDR(3)/MM proved a solution for formamide, difficulties arise in

the NMA spectrum, allowing essentially only for a meaningful comparison between band maxima and the experimental values.

For liquid water we find good agreement between experiment and theory for the lowest studied singlet excitation energy. The spectrum calculated using CCSDR(3)/MM energies is almost identical to the one calculated using CCSD/MM, implying negligible triples effects for this system.

Acknowledgment. This work has been supported by the Lundbeck Foundation and DCSC (Danish Center for Scientific Computing). O.C. acknowledges support from the Danish national research foundation, the Lundbeck Foundation, and EUROHORCs through a EURYI award. J.K. thanks the Villum Kann Rasmussen Foundation and the Danish Natural Science Research Council/The Danish Councils for Independent Research for financial support.

References

(1) Tomasi, J.; Persico, M. *Chem. Rev.* **1994**, *94*, 2027.

(2) Warshel, A.; Levitt, M. *J. Mol. Biol.* **1976**, *103*, 227.

(3) Singh, U.; Kollman, P. *J. Comput. Chem.* **1986**, *7*, 718.

(4) Kongsted, J.; Osted, A.; Mikkelsen, K. V.; Christiansen, O. *J. Chem. Phys.* **2003**, *118*, 1620.

(5) Kongsted, J.; Osted, A.; Mikkelsen, K. V.; Christiansen, O. The (Hyper)Polarizabilities of Liquid Water Modelled Using Coupled Cluster/Molecular Mechanics Response Theory Methods. In *Atoms, Molecules and Clusters in Electric Fields. Theoretical Approaches to the Calculation of Electric Polarizability*; Maroulis, G., Ed.; Imperial College Press: London, 2006.

(6) Kowalski, K.; Valiev, M. *J. Phys. Chem. A* **2006**, *110*, 13106.

(7) Fang, P.; Valiev, M.; Kowalski, K. *Chem. Phys. Lett.* **2008**, *458*, 205.

(8) Epifanovsky, E.; Kowalski, K.; Fan, P.-D.; Valiev, M.; Matsika, S.; Krylov, A. I. *J. Phys. Chem. A* **2008**, *112*, 9983.

(9) Hirata, S.; Yagi, K. *Chem. Phys. Lett.* **2008**, *464*, 123.

(10) Christiansen, O.; Koch, H.; Jørgensen, P. *Chem. Phys. Lett.* **1995**, *243*, 409.

(11) Christiansen, O.; Koch, H.; Jørgensen, P. *J. Chem. Phys.* **1995**, *103*, 7429–7441.

(12) Christiansen, O.; Koch, H.; Jørgensen, P.; Helgaker, T.; Olsen, J. *Chem. Phys. Lett.* **1996**, *256*, 185.

(13) Christiansen, O.; Koch, H.; Jørgensen, P. *J. Chem. Phys.* **1996**, *105*, 1451.

(14) Sauer, S. P. A.; Schreiber, M.; Silva-Junior, M. R.; Thiel, W. *J. Chem. Theory Comput.* **2009**, *5*, 555.

(15) Manohar, P. U.; Stanton, J. F.; Krylov, A. I. *J. Chem. Phys.* **2009**, *131*, 114112.

(16) Fukuda, R.; Hayaki, S.; Nakatsuji, H. *J. Chem. Phys.* **2009**, *131*, 174303.

(17) Watts, J. D.; Bartlett, R. J. *Spectrochim. Acta, Part A* **1999**, *55*, 495.

(18) Shiozaki, T.; Hirao, K.; Hirata, S. *J. Chem. Phys.* **2007**, *126*, 244106.

(19) Kowalski, K.; Piecuch, P. *J. Chem. Phys.* **2003**, *120*, 1715.

(20) Fujimoto, K.; Hayashi, S.; Hasegawa, J.; Nakatsuji, H. *J. Chem. Theory Comput.* **2007**, *3*, 605.

(21) Aidas, K.; Møgelhøj, A.; Nilsson, E. K.; Johnson, M. S.; Mikkelsen, K. V.; Christiansen, O.; Söderhjelm, P.; Kongsted, J. *J. Chem. Phys.* **2008**, *128*, 194503.

(22) Christiansen, O.; Nymand, T.; Mikkelsen, K. V. *J. Chem. Phys.* **2000**, *113*, 8101.

(23) Osted, A.; Kongsted, J.; Mikkelsen, K. V.; Aastrand, P. O.; Christiansen, O. *J. Chem. Phys.* **2006**, *124*, 124503.

(24) Helgaker, T.; Jørgensen, P.; Olsen, J. *Molecular Electronic Structure Theory*, 1st ed.; Wiley: New York, 2000.

(25) Christiansen, O.; Koch, H.; Halkier, A.; Jørgensen, P.; Helgaker, T.; de Meras, A. S. *J. Chem. Phys.* **1996**, *105*, 6921.

(26) Christiansen, O.; Mikkelsen, K. V. *J. Chem. Phys.* **1999**, *110*, 1365.

(27) Kendall, R. A.; Dunning, T. H.; Harrison, R. J. *J. Chem. Phys.* **1992**, *96*, 6796.

(28) Breneman, C. M.; Wiberg, K. B. *J. Comput. Chem.* **1990**, *11*, 361.

(29) Gagliardi, L.; Lindh, R.; Karlström, G. *J. Chem. Phys.* **2004**, *121*, 4494.

(30) Georg, H. C.; Coutinho, K.; Canuto, S. *J. Chem. Phys.* **2005**, *123*, 124307.

(31) Xie, W.; Pu, J.; MacKerell, A.; Gao, J. *J. Chem. Theory Comput.* **2007**, *3*, 1878.

(32) Linse, P. *MOLSIM, an integrated MD/MC/BD simulation program belonging to the MOLSIM package in C++*, 2004.

(33) Karlström, G.; Lindh, R.; Malmqvist, P.-Å.; Roos, B.; Ryde, U.; Veryazov, V.; Widmark, P.-O.; Cossi, M.; Schimmelpfennig, B.; Neogrady, P.; Seijo, L. *Comput. Mater. Sci.* **2003**, *28*, 222.

(34) Kongsted, J.; Osted, A.; Mikkelsen, K. V.; Christiansen, O. *Mol. Phys.* **2002**, *100*, 1813.

(35) Nielsen, C. B.; Christiansen, O.; Mikkelsen, K. V.; Kongsted, J. *J. Chem. Phys.* **2007**, *126*, 154112.

(36) *DALTON, a Molecular Electronic Structure Program, Release 2.0*, 2005; see http://www.kjemi.uio.no/software/dalton/dalton.html,

(37) *Midascpp, Molecular Interactions, Dynamics and Simulation Chemistry Program Package in C++*; http://www.chem.au.dk/∼midas (accessed Jan 6, 2010).

(38) Frisch, M. J.; Trucks, G. W.; Schlegel, H. B.; Scuseria, G. E.; Robb, M. A.; Cheeseman, J. R.; Montgomery, J. A., Jr.; Vreven, T.; Kudin, K. N.; Burant, J. C.; Millam, J. M.; Iyengar, S. S.; Tomasi, J.; Barone, V.; Mennucci, B.; Cossi, M.; Scalmani, G.; Rega, N.; Petersson, G. A.; Nakatsuji, H.; Hada, M.; Ehara, M.; Toyota, K.; Fukuda, R.; Hasegawa, J.; Ishida, M.; Nakajima, T.; Honda, Y.; Kitao, O.; Nakai, H.; Klene, M.; Li, X.; Knox, J. E.; Hratchian, H. P.; Cross, J. B.; Bakken, V.; Adamo, C.; Jaramillo, J.; Gomperts, R.; Stratmann, R. E.; Yazyev, O.; Austin, A. J.; Cammi, R.; Pomelli, C.; Ochterski, J. W.; Ayala, P. Y.; Morokuma, K.; Voth, G. A.; Salvador, P.; Dannenberg, J. J.; Zakrzewski, V. G.; Dapprich, S.; Daniels, A. D.; Strain, M. C.; Farkas, O.; Malick, D. K.; Rabuck, A. D.; Raghavachari, K.; Foresman, J. B.; Ortiz, J. V.; Cui, Q.; Baboul, A. G.; Clifford, S.; Cioslowski, J.; Stefanov, B. B.; Liu, G.; Liashenko, A.; Piskorz, P.; Komaromi, I.; Martin, R. L.;

Fox, D. J.; Keith, T.; Al-Laham, M. A.; Peng, C. Y.; Nanayakkara, A.; Challacombe, M.; Gill, P. M. W.; Johnson, B.; Chen, W.; Wong, M. W.; Gonzalez, C.; Pople, J. A. *Gaussian 03, Revision D.01*, Gaussian Inc.: Wallingford, CT, 2004.

(39) Losa, A. M.; Galvan, I. F.; Aguilar, M. A.; Martin, M. E. *J. Phys. Chem. B* **2007**, *111*, 9864.

(40) Bokareva, O. S.; Bataev, V. A.; Popyshev, V. I.; Godunov, I. A. *Spectr. Acta Part A* **2009**, *73*, 654.

(41) Adamo, C.; Barone, V. *Chem. Phys. Lett.* **1999**, *314*, 152.

(42) Heller, J. M.; Hamm, R. N.; Birkhoff, R. D.; Painter, L. R. *J. Chem. Phys.* **1974**, *60*, 3483.

(43) Petersen, C.; Dahl, N. H.; Jensen, S. K.; Poulsen, J. A.; Thøgersen, J.; Keiding, S. R. *J. Phys. Chem. A* **2008**, *112*, 3339.

(44) Besley, N. A.; Hirst, J. D. *J. Phys. Chem. A* **1998**, *102*, 10791.

(45) Rocha, W. R.; Martins, V. M.; Coutinho, K.; Canuto, S. *Theor. Chem. Acc.* **2002**, *108*, 31.

(46) Nielsen, E. B.; Schellman, J. A. *J. Phys. Chem.* **1967**, *71*, 2297.

(47) Rocha, W. R.; Almeida, K. J. D.; Coutinho, K.; Canuto, S. *Chem. Phys. Lett.* **2001**, *345*, 171.

(48) Gingell, J. M.; Mason, N. J.; Zhao, H.; Walker, I. C.; Siggel, M. R. F. *Chem. Phys.* **1997**, *220*, 191.

(49) Kaya, K.; Nagakura, S. *Theor. Chim. Acta.* **1967**, *7*, 124.

CT900641W